Electronic Supplementary Information

Effect of strong coordination bonds at axial or equatorial positions on magnetic relaxation for pentagonal bipyramidal dysprosium(III) single-ion magnets

Min Li,[a] Jiayi Han,[a] Haipeng Wu,[a]* Yien Du,[a] Yufang Liu,[a] Yongqiang Chen[a]* and Sanping Chen[b]*

[a] *Department of Chemistry and Chemical Engineering, Jinzhong University, Jinzhong, 030619, China.*

[b] *Key Laboratory of Synthetic and Natural Functional Molecule Chemistry of Ministry of Education, College of Chemistry and Materials Science, Northwest University, Xi'an, 710127, China*

Table S1. Crystal data and structure refinement summary for complexes **1-3**.

	1	2	3
Empirical formula	$C_{20}H_{24}Cl_3DyN_6O_4$	$C_{20}H_{22}Cl_2DyN_6O_3$	$C_{96}H_{92}Cl_9Dy_3N_{30}O_{28}$
Formula weight	681.3	627.83	2920.54
Crystal system	296.15	293(2)	293(2)
Temperature (K)	monoclinic	monoclinic	triclinic
Space group	$P2_1/c$	$P2_1/c$	$P\bar{1}$
a (Å)	9.6107(18)	9.6018(2)	11.2799(3)
b (Å)	22.067(4)	21.7017(5)	21.7618(6)
c (Å)	13.874(3)	13.7591(3)	25.8284(7)
α (°)	90	90	73.820(2)
β (°)	107.554(3)	107.146(2)	82.393(2)
γ (°)	90	90	82.882(2)
V (Å³)	2805.4(10)	2739.63(11)	6010.1(3)
Z	4	4	2
D_c (g m^{-3})	1.613	1.522	1.614
μ (mm^{-1})	2.984	16.636	12.368
F (000)	1340	1232	2906
Crystal size (mm)	0.16×0.14×0.12	0.15×0.13×0.13	0.14×0.06×0.05
Reflns	15119/5926	18089/4852	65718/21242
R_{int}	0.0675	0.0801	0.0783
GOF on F^2	1.0855	1.095	1.008
R_1[a] [$I > 2\sigma(I)$]	0.0691	0.0610	0.0625
wR_2[b] (all data)	0.1571	0.1557	0.1887
CCDC	2108069	2108068	2108070

[a]$R_1 = \Sigma(|| F_o | - | F_c ||)/\Sigma| F_o |$. [b]$wR_2 = [\Sigma w(F_o^2 - F_c^2)^2/\Sigma w(F_o^2)^2]^{1/2}$

Table S2 Selected bond lengths (Å) and bond angles (º) for **1-3**.

Complex **1**

Dy1-Cl1	2.599(2)	N3-Dy1-Cl1	86.59(19)
Dy1-Cl2	2.647(3)	N3-Dy1-Cl2	85.98(19)
Dy1-O1	2.150(4)	N3-Dy1-N1	133.0(2)
Dy1-N1	2.534(7)	N3-Dy1-N4	64.5(2)
Dy1-N3	2.503(7)	N3-Dy1-N2	67.8(2)
Dy1-N4	2.536(7)	N4-Dy1-Cl1	95.98(19)
Dy1-N2	2.505(7)	N4-Dy1-Cl2	87.68(19)
Cl1-Dy1-Cl2	169.34(9)	N2-Dy1-Cl1	84.3(2)
O1-Dy1-Cl1	101.30(17)	N2-Dy1-Cl2	85.8(2)
O1-Dy1-Cl2	89.20(18)	N2-Dy1-N1	65.2(2)
O1-Dy1-N1	83.0(2)	N2-Dy1-N4	132.1(2)
O1-Dy1-N3	143.7(2)	N1-Dy1-Cl1	88.25(19)
O1-Dy1-N4	79.4(2)	N1-Dy1-Cl2	91.25(19)
O1-Dy1-N2	147.6(2)	N1-Dy1-N4	162.4(2)

Complex **2**

Dy1-Cl1	2.593(2)	N4-Dy1-Cl1	88.22(18)
Dy1-Cl2	2.637(2)	N4-Dy1-Cl2	90.69(19)
Dy1-O1	2.131(6)	N4-Dy1-N1	162.9(2)
Dy1-N1	2.542(7)	N2-Dy1-Cl2	87.31(17)
Dy1-N2	2.498(6)	N2-Dy1-N1	63.9(2)
Dy1-N3	2.513(7)	N2-Dy1-N3	68.1(2)
Dy1-N4	2.537(7)	N2-Dy1-N4	133.1(3)
Cl1-Dy1-Cl2	171.36(10)	N3-Dy1-Cl1	85.07(19)
O1-Dy1-Cl1	96.91(18)	N3-Dy1-Cl2	86.70(19)
O1-Dy1-Cl2	91.44(19)	N3-Dy1-N1	131.8(2)
O1-Dy1-N1	80.6(2)	N3-Dy1-N4	65.0(3)
O1-Dy1-N2	144.5(2)	N1-Dy1-Cl1	96.11(18)

O1-Dy1-N3	147.3(2)	N1-Dy1-Cl2	87.42(19)
O1-Dy1-N4	82.4(2)	N2-Dy1-Cl1	87.18(17)

Complex **3**

Dy2-O20	2.192(4)	O17-Dy2-N15	147.8(2)
Dy2-O17	2.169(5)	O14-Dy2-O20	172.5(2)
Dy2-O14	2.177(4)	O14-Dy2-N13	85.46(18)
Dy2-N13	2.550(6)	O14-Dy2-N14	91.5(2)
Dy2-N14	2.543(7)	O14-Dy2-N16	90.7(2)
Dy2-N16	2.553(7)	O14-Dy2-N15	83.1(2)
Dy2-N15	2.530(7)	N13-Dy2-N16	162.3(2)
Dy1-O11	2.176(4)	N14-Dy2-N13	64.7(2)
Dy1-O6	2.169(5)	N14-Dy2-N16	132.8(2)
Dy1-O1	2.190(5)	N15-Dy2-N13	130.1(2)
Dy1-N1	2.546(6)	N15-Dy2-N14	67.3(2)
Dy1-N4	2.564(6)	N15-Dy2-N16	66.2(3)
Dy1-N3	2.520(6)	O6-Dy1-N3	146.6(2)
Dy1-N2	2.514(7)	O6-Dy1-N2	145.4(2)
Dy3-O23	2.210(5)	O1-Dy1-N1	99.5(2)
Dy3-O31	2.171(5)	O1-Dy1-N4	85.2(2)
Dy3-N24	2.515(6)	O1-Dy1-N3	89.5(2)
Dy3-N23	2.533(7)	N24-Dy3-N23	64.8(2)
Dy3-O28	2.216(7)	O28-Dy3-N24	142.4(2)
Dy3-N25	2.489(8)	O28-Dy3-N23	79.7(3)
Dy3-N26	2.497(9)	N26-Dy3-N23	159.9(3)
O17-Dy2-N16	81.6(2)	O1-Dy1-N2	84.7(3)
O11-Dy1-O1	171.0(2)	N1-Dy1-N4	163.4(2)
O11-Dy1-N1	87.68(19)	N3-Dy1-N1	130.7(2)
O11-Dy1-N4	89.44(19)	O23-Dy3-N23	99.0(2)

O11-Dy1-N3	81.7(2)	O23-Dy3-O28	89.1(2)
O11-Dy1-N2	93.6(2)	O23-Dy3-N25	87.3(2)
O6-Dy1-O11	95.0(2)	O20-Dy2-N13	95.28(19)
O6-Dy1-O1	91.5(3)	O20-Dy2-N14	82.1(2)
N2-Dy1-N1	64.9(2)	O20-Dy2-N16	90.7(2)
N2-Dy1-N4	131.6(2)	O20-Dy2-N15	90.8(2)
N2-Dy1-N3	67.9(2)	O17-Dy2-O20	89.7(2)
O23-Dy3-N24	84.8(2)	O17-Dy2-O14	97.8(2)
O23-Dy3-N26	89.5(3)	O17-Dy2-N13	81.8(2)
O6-Dy1-N1	82.0(2)	O17-Dy2-N14	144.4(2)
O6-Dy1-N4	82.0(2)	O31-Dy3-O23	170.7(2)
N3-Dy1-N4	64.8(2)	O31-Dy3-N24	90.6(2)
O28-Dy3-N25	147.9(3)	O31-Dy3-N23	86.3(2)
O28-Dy3-N26	82.3(4)	O31-Dy3-O28	99.4(2)
N25-Dy3-N24	69.0(2)	O31-Dy3-N25	83.5(2)
N25-Dy3-N23	132.4(3)	O31-Dy3-N26	87.9(2)
N25-Dy3-N26	65.8(4)	N26-Dy3-N24	134.6(3)

Table S3. Shape analysis for the metal centers of complexes **1-3.**

complex **1**	HPY-7	PBPY-7	COC-7	CTPR-7	JPBPY-7	JETPY-7
Dy1	26.147	0.679	8.327	6.483	5.487	23.929

complex **2**	HPY-7	PBPY-7	COC-7	CTPR-7	JPBPY-7	JETPY-7
Dy1	25.932	0.664	7.916	6.140	5.456	23.471

complex **3**	HPY-7	PBPY-7	COC-7	CTPR-7	JPBPY-7	JETPY-7
Dy1	22.968	1.260	5.720	4.655	2.957	22.627

Dy2	24.039	1.137	6.133	4.937	2.821	21.925
Dy3	23.701	1.018	6.345	4.738	2.822	21.708

HPY-7 (C_{6v}): Hexagonal pyramid
PBPY-7 (D_{5h}): Pentagonal bipyramid
COC-7 (C_{3v}): Capped octahedron
CTPR-7 (C_{2v}): Capped trigonal prism
JPBPY-7 (D_{5h}): Johnson pentagonal bipyramid J13
JETPY-7 (C_{3v}): Johnson elongated triangular pyramid J7

Table S4. Deviations (Å) from the ideal plane defined by five coordination atoms for **1-3**. The positive value denotes that the atom is located on the same side of the Ln atom, whereas a negative value denotes that the atom is located on the opposite side.

		1		2		3
Coordination	N1	0.0560	N1	-0.0323	N1	0.1890
atoms	N2	-0.0514	N2	0.0445	N2	-0.2464
	N3	0.0212	N3	-0.0359	N3	0.1865
	N4	0.0168	N4	0.0127	N4	-0.0502
	O1	-0.0426	O1	0.0111	O4	-0.0788
r.m.s. deviation		0.0408		0.0303		0.1673

Table S5 charge distributions for ligand atoms used as input for Magellan (the partial charges of the donor atoms were estimated based on the literature and used in the input file)[1].

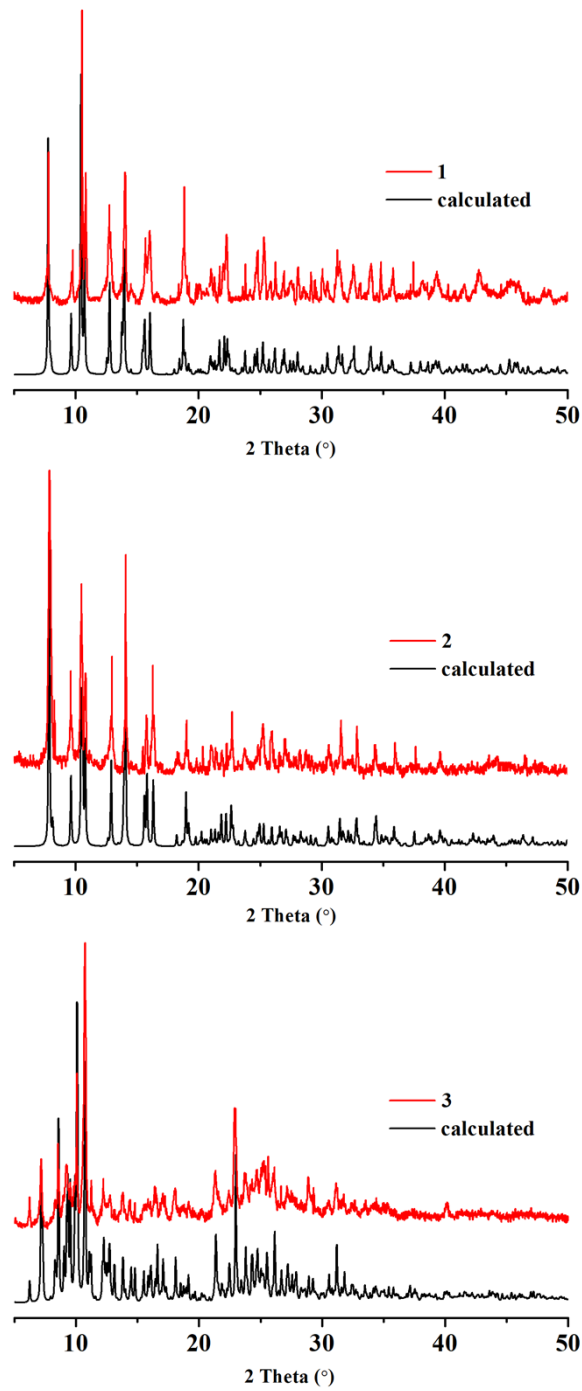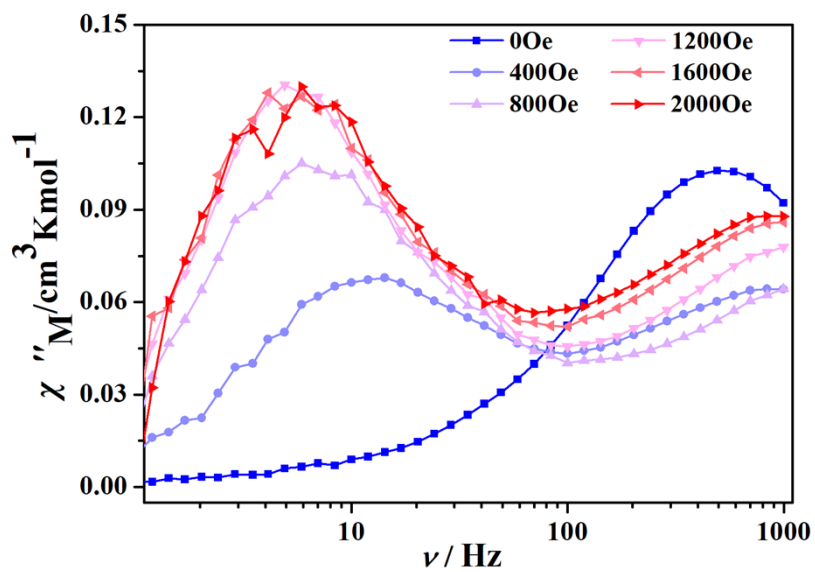| 1		2		3	
Dy1	3	Dy1	3	Dy1	3
Cl1	-0.85	Cl1	-0.85	O1	-0.85
Cl2	-0.85	Cl2	-0.85	O6	-0.85
O1	-0.85	O1	-0.85	O11	-0.85
N1	-0.35	N1	-0.35	N1	-0.35
N2	-0.4	N2	-0.4	N2	-0.4
N3	-0.4	N3	-0.4	N3	-0.4
N4	-0.35	N4	-0.35	N4	-0.35

Fig. S1 PXRD curves for **1-3**.

Fig. S2. Field dependence of the out-of-phase signal *vs* frequency at 8 K for **1**.
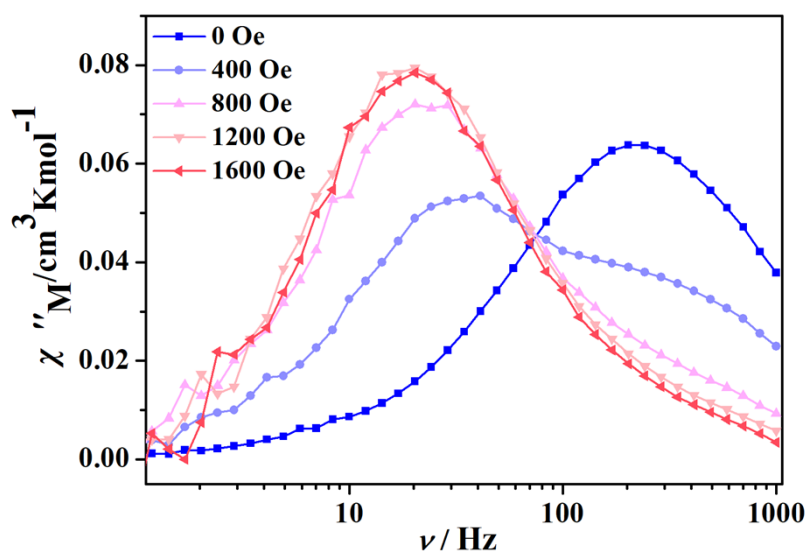

Fig. S3. Field dependence of the out-of-phase signal *vs* frequency at 8 K for **2**.
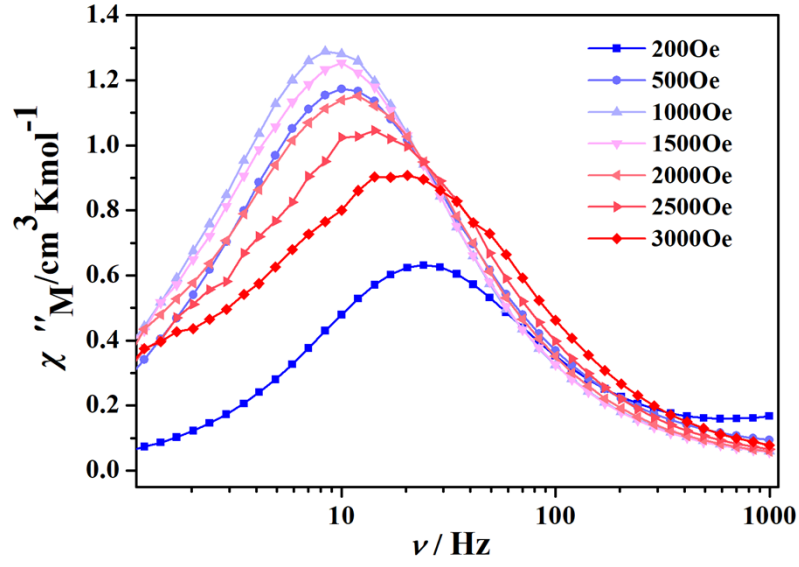
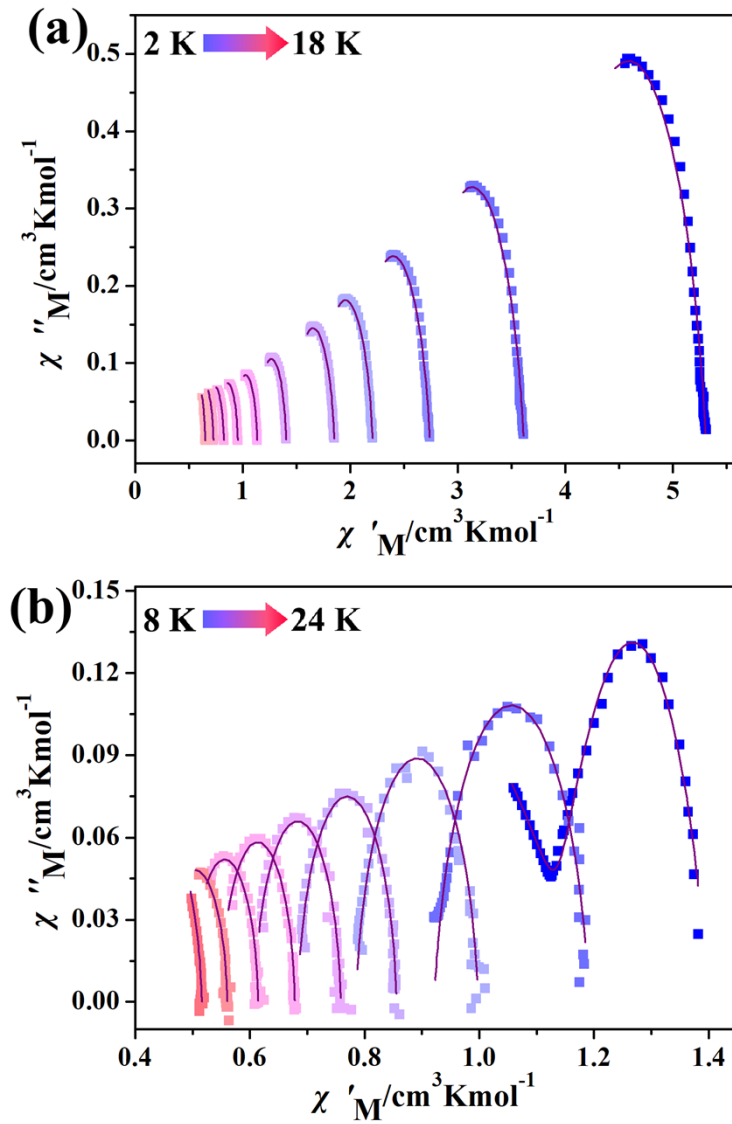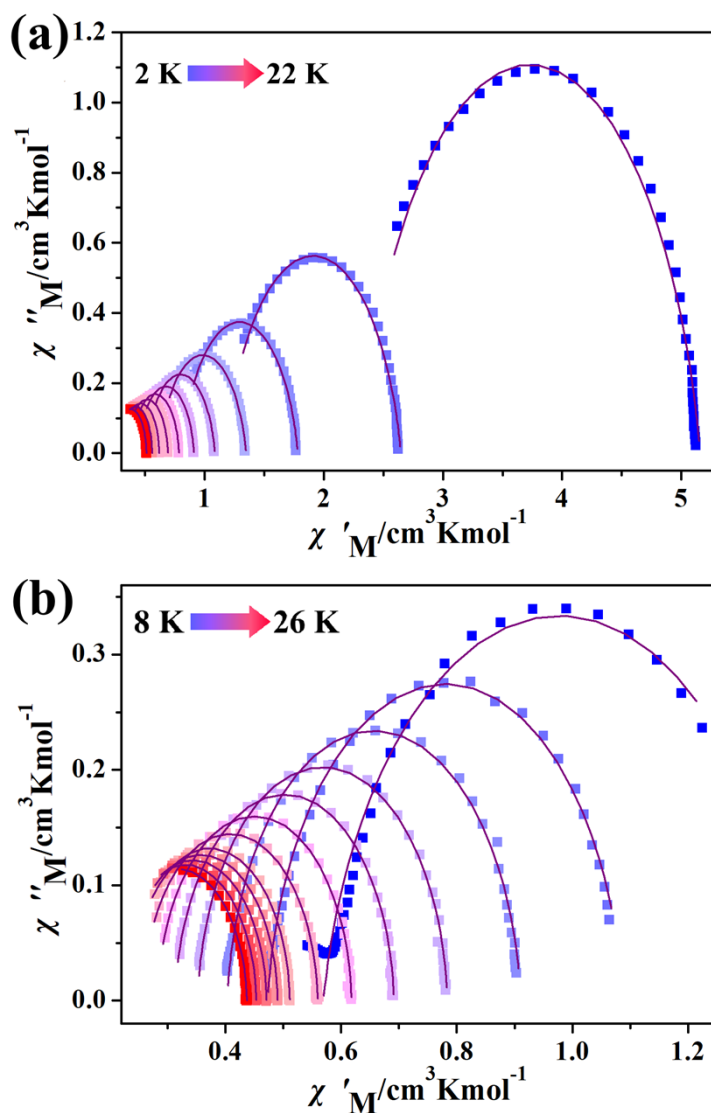**Fig. S4**. Field dependence of the out-of-phase signal *vs* frequency at 8 K for **3**.

Fig. S5 Cole-Cole plots using the frequency-dependence ac susceptibility data under (a) zero and (b) 1200 Oe dc field for **1**. The solid lines correspond to the best fits.

Fig. S6 Cole-Cole plots using the frequency-dependence ac susceptibility data under (a) zero and (b) 1200 Oe dc field for **2**. The solid lines correspond to the best fits obtained by the generalized Debye model.
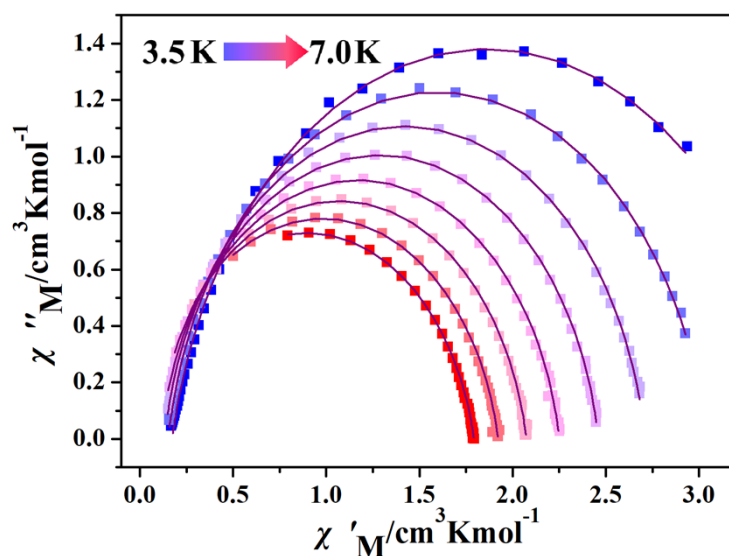
Fig. S7 Cole-Cole plots using the frequency-dependence ac susceptibility data under 1000 Oe dc field for **3**. The solid lines correspond to the best fits obtained by the generalized Debye model.
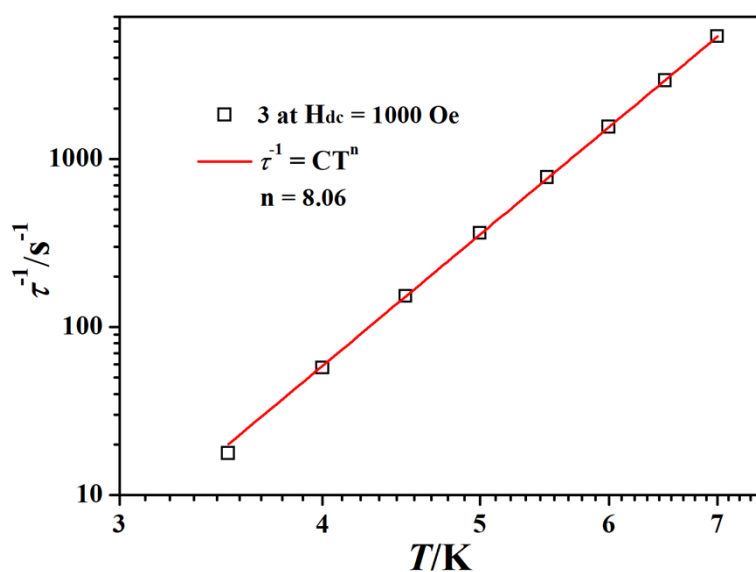

Fig. S8 log-log plots of τ^{-1} *vs. T* under 1000 Oe dc fields for **3**. The solid lines represent the best fit.

References

1 H. Wu, M. Li, B. Yin, Z. Xia, H. Ke, Q. Wei, G. Xie, S. Chen and S. Gao, *Dalton trans.*, 2019, **48**, 16384-16394.